



Advanced glycation endproducts increase proliferation, migration and invasion of the breast cancer cell line MDA-MB-231

Hana Sharaf ^{a,1}, Sabine Matou-Nasri ^{b,1}, Qiyu Wang ^a, Zaki Rabban ^b, Hamad Al-Eidi ^b, Abdulkareem Al Abdulrahman ^b, Nessim Ahmed ^{a,*}

^a School of Healthcare Science, Manchester Metropolitan University, Manchester M1 5GD, United Kingdom

^b King Abdullah International Medical Research Center, Medical Genomics Research Department, National Guard Health Affairs, Riyadh 11426, Saudi Arabia



ARTICLE INFO

Article history:

Received 21 March 2014

Received in revised form 17 November 2014

Accepted 9 December 2014

Available online 13 December 2014

Keywords:

Advanced glycation endproduct

Diabetes

Breast cancer

Signaling pathway

Methylglyoxal

ABSTRACT

Diabetic patients have increased likelihood of developing breast cancer. Advanced glycation endproducts (AGEs) underlie the pathogenesis of diabetic complications but their impact on breast cancer cells is not understood. This study aims to determine the effects of methylglyoxal-derived bovine serum albumin AGEs (MG-BSA-AGEs) on the invasive MDA-MB-231 breast cancer cell line. By performing cell counting, using wound-healing assay, invasion assay and zymography analysis, we found that MG-BSA-AGEs increased MDA-MB-231 cell proliferation, migration and invasion through MatriGel™ associated with an enhancement of matrix metalloproteinase (MMP)-9 activities, in a dose-dependent manner. Using Western blot and flow cytometry analyses, we demonstrated that MG-BSA-AGEs increased expression of the receptor for AGEs (RAGE) and phosphorylation of key signaling protein extracellular signal-regulated kinase (ERK)-1/2. Furthermore, in MG-BSA-AGE-treated cells, phospho-protein micro-array analysis revealed enhancement of phosphorylation of the ribosomal protein 70 serine S6 kinase beta 1 (p70S6K1), which is known to be involved in protein synthesis, the signal transducer and activator of transcription (STAT)-3 and the mitogen-activated protein kinase (MAPK) p38, which are involved in cell survival. Blockade of MG-BSA-AGE/RAGE interactions using a neutralizing anti-RAGE antibody inhibited MG-BSA-AGE-induced MDA-MB-231 cell processes, including the activation of signaling pathways. Throughout the study, non-modified BSA had a negligible effect. In conclusion, AGEs might contribute to breast cancer development and progression partially through the regulation of MMP-9 activity and RAGE signal activation. The up-regulation of RAGE and the concomitant increased phosphorylation of p70S6K1 induced by AGEs may represent promising targets for drug therapy to treat diabetic patients with breast cancer.

© 2014 Elsevier B.V. All rights reserved.

1. Introduction

Diabetes and cancer are major health problems and prevalent diseases with a globally increasing incidence. Generally, cancer has an increased metabolism associated with elevated glycolytic rates which enhance the formation of advanced glycation endproducts (AGEs) [1].

Abbreviations: AGE, Advanced glycation endproduct; AP, Activator protein; BSA, Bovine serum albumin; DMEM, Dulbecco's modified Eagle's medium; EDTA, Ethylenediaminetetraacetic acid; ERK, Extracellular-signal regulated kinase; FBS, Fetal bovine serum; JNK, c-jun kinase; RAGE, Receptor for advanced glycation endproducts; MAPK, Mitogen-activated protein kinase; MG, Methylglyoxal; MG-BSA-AGES, Methylglyoxal-derived bovine serum albumin AGEs; MMP, Matrix metalloproteinase; NF- κ B, Nuclear factor kappa B; PI3K, Phosphoinositol-3 kinase; PKC, Protein kinase C; PMSF, Phenylmethylsulfonyl fluoride; p70S6K1, Ribosomal protein 70 serine S6 kinase beta 1; ROS, Reactive oxygen species; SD, Standard deviation; SDS-PAGE, Sodium dodecyl sulfate polyacrylamide gel electrophoresis; SPM, Serum-poor medium; STAT, Signal transducer and activator of transcription

* Corresponding author. Tel.: +44 161 247 1163; fax: +44 161 247 6831.

E-mail address: N.Ahmed@mmu.ac.uk (N. Ahmed).

¹ Contributed equally.

AGEs are a group of heterogeneous macromolecules formed during a non-enzymatic reaction called the Maillard reaction [2]. This Maillard reaction is responsible for the intermolecular cross-linking between the reactive carbonyl group of sugars and the nucleophilic amino group of proteins, lipids or nucleic acids [3,4]. Although this glycation reaction is a non-specific biochemical reaction, protein modification results in altered enzyme activity [5], immunogenicity [6], decreases ligand binding [7], and cross-linking of extracellular matrix proteins, which cause stiffening [8]. Increased protein glycation has been associated with several age-related [9] and chronic inflammatory diseases such as cardiovascular diseases [10], Alzheimer's disease [11], stroke, retinopathy [12], nephropathy [13], neuropathy and cancer [14]. In addition, AGE formation is often accompanied by increased free radical activity, which can damage cell membranes and cause gene mutations resulting in malignant cell transformation [15].

The cellular effects of AGEs are mainly mediated through the receptor for advanced glycation endproducts (RAGE). RAGE is a 45-kDa transmembrane multi-ligand signal transduction receptor belonging to the immunoglobulin superfamily, which is highly expressed during embryonic

development, especially in the brain, and then its expression decreases in adult tissues [16]. In pathological conditions, RAGE expression is induced by high glucose [17], reactive oxygen species (ROS), external stress, hypoxia [18], pro-inflammatory mediators and by AGE itself [17]. RAGE is also over-expressed on activated immune cells [19], vascular cells [20] and cancer cells [21]. AGE–RAGE interactions trigger a diverse array of signaling pathways [22], including mitogen activated protein kinase (MAPK) such as extracellular-signal regulated kinase (ERK)-1/2 [20], p38 [23] and c-jun kinase (JNK), that induce the activation of transcription factors such as nuclear factor kappa B (NF- κ B) [24], activator protein (AP)1 and signal transducers and activators of transcription (STAT)-3 [25]. This is accompanied by ROS production [26] and by subsequent transcription and changes in gene expression, which result in tumor growth through increased cell proliferation [27] and tumor metastasis through stimulation of cell migration and invasion [14]. In addition, matrix metalloproteinases (MMPs) and especially gelatinases (i.e. MMP-2 and MMP-9) are known to promote cancer progression with their central role during the invasion process as they degrade the connective tissue mainly composed of type I collagen (or gelatine for denatured collagen) and the

basement membrane mainly composed of type IV collagen [28]. AGE–RAGE interactions also induce the activation of phosphoinositol-3 kinase (PI3K) [27], oncogenic Ras, protein kinase C (PKC) and members of Rho/GTPase (Cdc42 and Rac-1) signaling pathways, which lead to cell survival, stress responses and apoptosis, release of growth factors and pro-inflammatory cytokines, and motility with changes in cell shape, respectively [29].

A meta-analysis study has reported that breast cancer rates are increased by 23% for women who are diagnosed with type 2 diabetes [30]. Breast cancer is a heterogeneous disease of particular interest. It is classified into different subtypes based on expression of hormone (oestrogen and progesterone) receptors and on its capability to invade, which defines the degree of the malignancy. Much attention has been devoted to the most aggressive phenotype of breast cancer with the identification of the roles of AGEs and the increase of RAGE expression in patient's tissues [31]. However, biological effects of AGEs–RAGE on breast cancer cells are poorly investigated. Here, in an attempt to understand the biological effects of AGEs/RAGE in breast cancer, we investigated the effects of methylglyoxal-derived bovine serum albumin

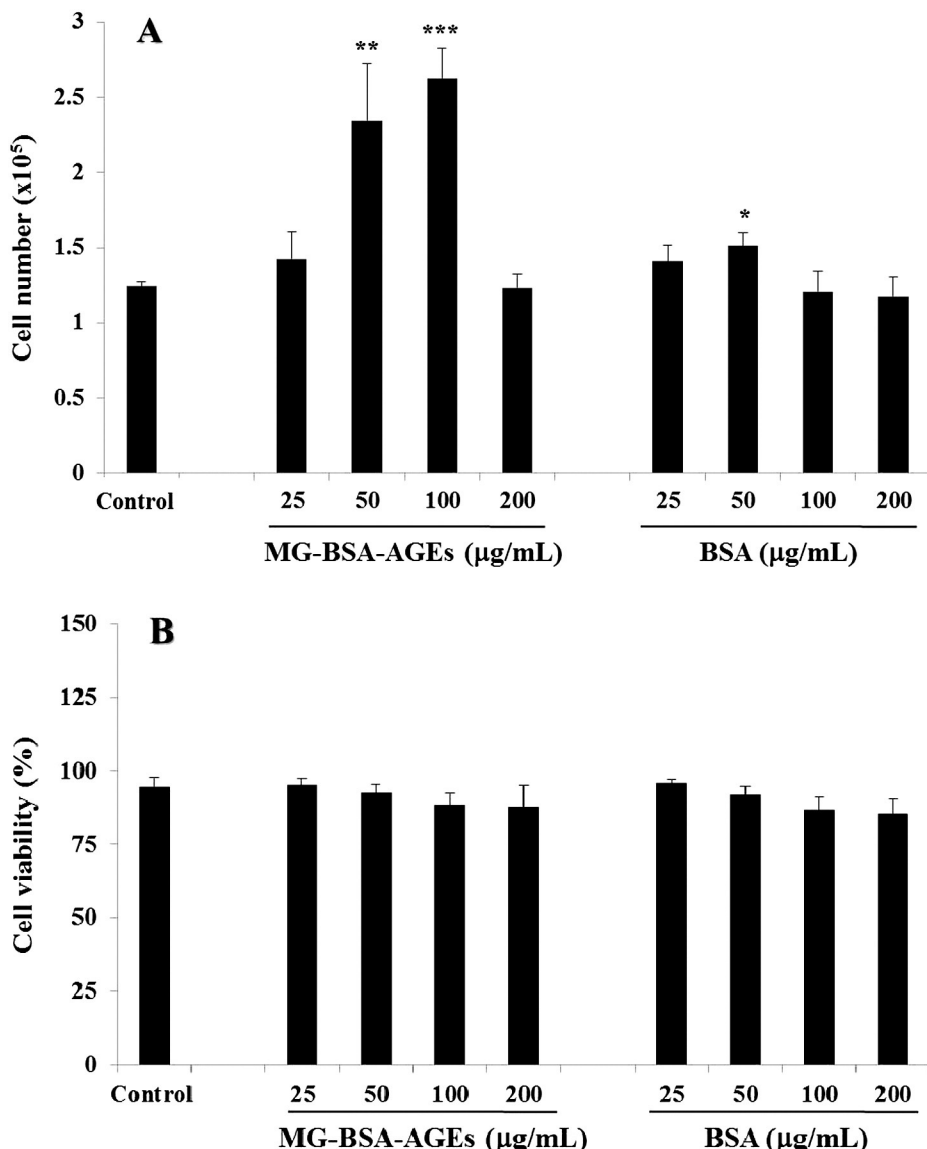


Fig. 1. Effect of MG-BSA-AGEs and non-modified BSA on (A) the proliferation and (B) the viability of breast cancer MDA-MB-231 cells. Cells were treated for 72 h of incubation with 25–200 μ g/ml MG-BSA-AGEs or non-modified BSA. Cell number (A) and cell viability (B) were determined using an automatic cell counter and the trypan blue exclusion method, respectively. Control indicates non-treated cells. Results are presented as mean \pm SD of three independent experiments. (*), (**) and (***) signify a statistically significant difference ($p < 0.05$, $p < 0.01$ and $p < 0.001$), compared with the control.

AGES (MG-BSA-AGEs) on an invasive and non-hormone-dependent breast cancer cell line MDA-MB-231, with regard to cell proliferation, migration and invasion. The signaling pathways underlying the MG-BSA-AGE-mediated effects were also investigated. To determine the consequences of glycation on MDA-MB-231 cell functions, the biological effects of non-modified BSA were also determined.

2. Materials and methods

2.1. Reagents

All reagents were obtained from Sigma-Aldrich (Dorset, UK) unless mentioned otherwise.

2.2. Preparation of MG-BSA-AGEs

Bovine serum albumin (BSA) fraction V (10 mg/ml) was incubated with 0.1 M methylglyoxal (MG) in 0.1 M sodium phosphate buffer containing 3 mM sodium azide (pH 7.4) and left at 37 °C for 72 h. This glycated BSA was dialyzed against distilled water to remove unbound sugars. Dialysis was performed by stirring the samples at 4 °C with daily changes of distilled water until equilibrium was reached. Non-modified BSA underwent the same preparation conditions but in the absence of MG. The resulting MG-BSA-AGEs were characterized using a fluorescence spectrophotometer (Luminescence spectrometer model LS 30 from Perkin Elmer LAS Ltd., Buckinghamshire, UK) with emission at 420 nm after excitation at 350 nm, which confirmed the higher intensity of MG-BSA-AGEs than that of non-modified BSA. Bacterial endotoxins were removed from non-modified BSA and MG-BSA-AGE solutions using detoxi-gel endotoxin-removing gel columns (Thermo Scientific, Rockford, USA). Endotoxin levels in MG-BSA-AGEs and non-modified BSA solutions were measured with an E-toxate kit based on the *Limulus Amebocyte lysate* assay and were found to be below the detection limit (<0.125 EU/ml). Protein concentrations were determined using a

Bradford-based assay (Bio-Rad Laboratories, Hertfordshire, UK) with BSA as a standard.

2.3. Culture of MDA-MB-231 breast cancer cells

MDA-MB-231 breast cancer cell line was obtained from American Type Culture Collection (Manassas, VA, USA) and cultured in complete medium composed of Dulbecco's modified Eagle's medium (DMEM) supplemented with 10% heat-inactivated fetal bovine serum (FBS), 2 mM glutamine and antibiotics (100 µg/ml streptomycin, 100 IU/ml penicillin) at 37 °C in a saturated air humidity/5% CO₂ incubator.

2.4. Cell proliferation assay

MDA-MB-231 cells (2.5×10^4 /ml) were seeded in complete medium in 24-well plates (Nunc™, Fisher Scientific, Loughborough, UK). After 4 h of incubation to allow the cells to attach to the bottom of the well, the medium was changed to a serum-poor medium (SPM) supplemented with 2.5% FBS in the presence or absence of different concentrations (25–200 µg/ml) of MG-BSA-AGEs or non-modified BSA. Each condition was performed in triplicate. After 72 h of incubation, the cells were detached in 250 µl of 0.05% trypsin/0.02% EDTA, and each cell suspension was diluted in 10 ml of isotonic solution and counted using a Beckman-Coulter counter (Buckinghamshire, UK). Cell viability was assessed using the trypan blue exclusion method, which stains dead cells; whereas viable cells actively exclude the dye. The percentage of cell viability was determined according to the following formula: % viability = (viable unstained cells)/(viable unstained cells + dead stained cells) × 100.

2.5. Cell migration assay

MDA-MB-231 cells (5×10^4 /ml) were seeded in complete medium on Thermanox® plastic coverslips (Nunc™) in 24-well plates. After 24 h of incubation, the cells reached pre-confluence on the coverslips;

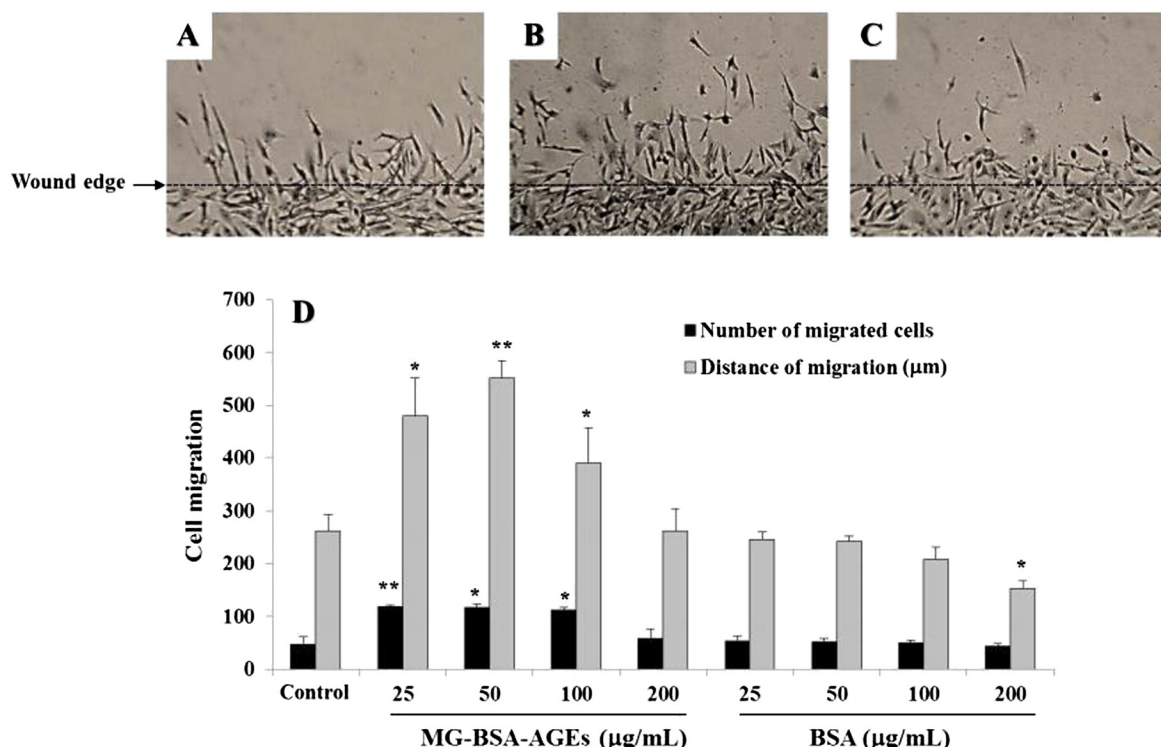


Fig. 2. Effect of MG-BSA-AGEs and non-modified BSA on the migration of breast cancer MDA-MB-231 cells. Representative photomicrographs ($\times 400$ magnification) showing MDA-MB-231 cell migration measured from the wound edge (indicated by the arrow) after 24 h of incubation in (A) non-treated (control) or (B) 50 µg/ml MG-BSA-AGE-treated or (C) non-modified BSA-treated cells. Scale bar = 100 µm. (D) Quantification of the number of migrated cells (black bars) and the distance of migration (gray bars) of MDA-MB-231 cells treated in the aforementioned conditions. Results are presented as mean \pm SD of three independent experiments. (*) and (**) signify a statistically significant difference ($p < 0.05$ and $p < 0.01$), compared with the control.

the culture medium was changed to SPM for a further 24-h incubation. At confluence, cells were washed three times with sterile PBS, and each monolayer was wounded on two sides with a sterile razor blade, which formed two wound edges per coverslip with cell denuded areas. Dislodged cells and cell debris were removed with sterile PBS. The coverslips with wounded cell monolayers were returned to the well containing SPM with or without different concentrations of MG-BSA-AGEs and non-modified BSA for 24 h of incubation. Each condition was performed in duplicate. At the end of the experiment, the cells were rinsed with PBS, fixed with 100% ethanol for 5 min and then left to dry at room temperature. The cells were stained with 0.1% methylene blue for 2 min and washed abundantly with distilled water to reveal the degree of wound recovery. Four pictures from the wound edge of each side were taken to assess the cell migration by counting the number of the migrated cells and by measuring the distance of the cell migration using image J software (<http://rsbweb.nih.gov/ij/index.html>).

2.6. Cell invasion Matrigel™ assay

Growth-factor reduced Matrigel™ (Becton Dickinson, Oxford, UK) was diluted (1:6) in serum-free medium then poured onto the porous membrane of a Transwell® 24-insert plate (Nunc™). The plate was incubated for 30 min to allow the gel to polymerise. MDA-MB-231 cells were seeded at 10^4 cells/100 μ l in SPM (in the upper chamber of the Transwell®) in the presence or absence of different concentrations of MG-BSA-AGEs or non-modified BSA (in the well corresponding to the lower chamber of the Transwell®). Each condition was performed

in duplicate. After 24 h of incubation, the non-migrated cells on the upper side of the porous membrane were removed using a cotton swab soaked with PBS. The cells that migrated across the porous membrane were fixed with 4% paraformaldehyde and then stained with 0.1% Giemsa stain for cell counting using a Zeiss optical microscope.

2.7. Gelatine zymography

Matrix metalloproteinase (MMP) activities in the cell-culture media that had been used for the cell invasion assay (as aforementioned) were measured. The medium was collected and centrifuged (600g for 15 min at 4 °C). Protein concentration was determined using the Bradford protein assay (Bio-Rad), and the samples (100 μ g of protein) were mixed with an equal volume of non-reducing sample buffer. The samples were incubated at room temperature for 10 min, after which they were subjected to electrophoresis on 7.5% sodium dodecyl sulfate-polyacrylamide gel electrophoresis (SDS-PAGE) containing 1 mg/ml gelatine as a substrate. The gels were washed in re-naturation buffer (2.5% Triton X-100) for 30 min at room temperature to remove SDS and to re-nature the MMPs in the gels. The gels were then rinsed in activation buffer (50 mM Tris-HCl, 0.2 M NaCl, 5 mM CaCl₂ and 0.02% Brij 35) for 30 min to activate the MMPs. Gels were incubated overnight at 37 °C with fresh activation buffer and stained with 0.5% Coomassie blue R-250 for 2 h at room temperature. After destaining the gels, MMP gelatinase activity was detected as a white band on a dark background and quantified by densitometry using Image J software.

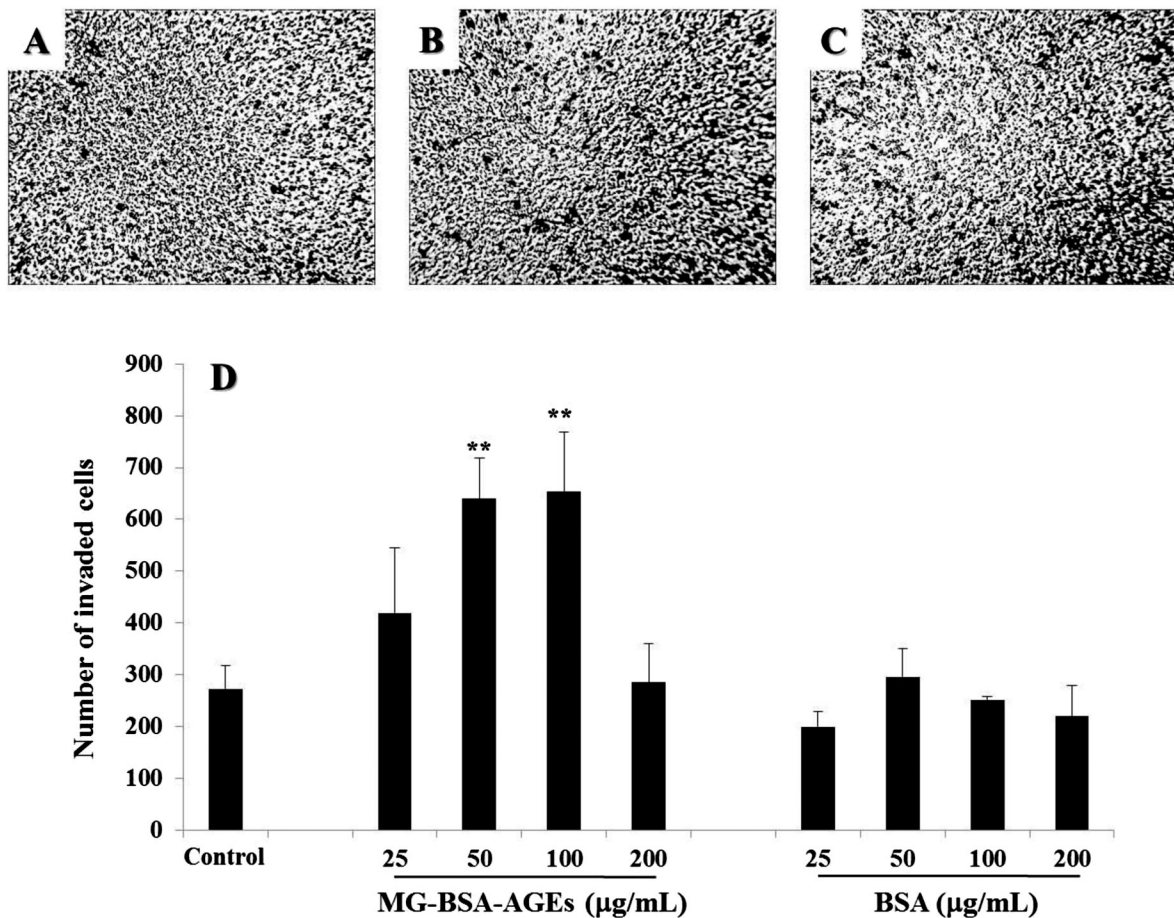


Fig. 3. Effect of MG-BSA-AGEs and non-modified BSA on the invasion of breast cancer MDA-MB-231 cells. Representative photomicrographs ($\times 100$ magnification) of (A) untreated MDA-MB-231 cells (control), (B) cells treated with 100 μ g/ml MG-BSA-AGEs and (C) non-modified BSA in the Matrigel™ invasion assay. Stimulated cells which had invaded the Matrigel™ (a reconstituted basement membrane) and migrated across the porous membrane were stained with Giemsa dye for counting. (D) Quantification of number of invaded MDA-MB-231 cells after treatment with 25–200 μ g/ml MG-BSA-AGEs or non-modified BSA, compared with the control. Results are presented as mean \pm SD of three independent experiments. (**) signifies a statistically significant difference ($p < 0.01$), compared with the control.

2.8. Preparation of cell lysates and Western blot analysis

MDA-MB-231 cells (6×10^5 /2 ml) were seeded in complete medium in six-well plates (Nunc™). After 48 h of incubation, the medium was renewed with SPM for a further 24-h incubation, and MG-BSA-AGEs or non-modified BSA was added for 5, 10, 30 and 120 min of incubation. After washing in cold PBS, all the intracellular proteins were extracted after lysing the cells with 120 μ l/well of ice-cold radioimmunoprecipitation buffer (pH 7.5) containing 25 mM Tris-HCl, 150 mM NaCl, 0.5% sodium deoxycholate, 0.5% SDS, 1 mM EDTA, 1 mM sodium orthovanadate, 1 mM phenylmethylsulfonyl fluoride (PMSF), 1% Triton X-100 and 1 μ M leupeptin.

For a time-course study of RAGE expression, the cells were treated with or without MG-BSA-AGEs or non-modified BSA for 10 min and 24–72 h of incubation. The cells were then lysed with 80 μ l/well of ice-cold buffer containing 10 mM Tris-HCl (pH 7.4), 50 mM NaCl, 5 mM EDTA, 1% Triton X-100, 0.05% SDS, 50 mM sodium fluoride, 100 μ M sodium orthovanadate, 10 mM beta-glycerophosphate, 10 mM sodium pyrophosphate, 100 μ g/ml PMSF, 3 mM benzamidine, 1 mM dithiothreitol, 10 μ M leupeptin, 5 μ M pepstatin A and a cocktail of protease inhibitors. Protein lysates (100 μ g) were mixed with 2 \times Laemmli sample buffer, denatured by boiling in a water bath for 15 min and then centrifuged.

To remove the cell debris, the cell lysates were centrifuged at 20,000 g for 30 min at 4 °C. The amount of proteins for each sample was determined by Bio-Rad protein assay and was fixed at 20–50 μ g for equal protein loading. An equal volume of protein samples and 2 \times sample buffer were mixed in Eppendorf® tubes and then placed in the boiling water for 15 min. Samples were separated along with pre-stained molecular weight markers by 12% SDS-PAGE. Proteins were electroblotted onto nitrocellulose membranes and the membranes were blocked for 1 h at room temperature in Tris-buffered saline (TBS)-Tween (pH 7.4) containing 1% BSA. Membranes were stained with the following primary antibodies diluted in the blocking buffer, overnight at 4 °C on a rotating shaker: mouse monoclonal antibodies to phospho-extracellular signal-

regulated kinase (p-ERK1/2, Tyr204 of ERK1, sc-7976; 1:1000 dilution), rabbit polyclonal antibodies to total ERK1/2 [C-16] (t-ERK1/2, sc-93; 1:1000 dilution) and mouse monoclonal antibodies to RAGE [E-1] (sc-74473; 1:1000 dilution) provided by Santa Cruz Biotechnology (Heidelberg, Germany) and mouse monoclonal antibodies to GAPDH [6C5] (ab8245; 1:2000 dilution) and to p70S6K1 [6B2] (ab119252; 1:1000) and rabbit monoclonal antibodies to phospho-p70S6K1 (p-p70S6K1, Tyr412, ab78413; 1:1000) by Abcam (Cambridge, UK). After washing five times for 10 min in TBS-Tween at room temperature, the membranes were stained with either rabbit anti-mouse or goat anti-rabbit horseradish peroxidase-conjugated secondary antibodies diluted in TBS-Tween containing 5% de-fatted milk (1:1000 dilution) for 1 h at room temperature with continuous mixing. After a further five washes in TBS-Tween, proteins were visualized using ECL chemiluminescent detection (Amersham Biosciences, Buckinghamshire, UK) and analyzed using GeneSnap software with Gene tool image analyser (Syngene, Cambridge, UK).

2.9. RNA extraction and real-time RT-PCR

MDA-MB-231 cells (6×10^5 /2 ml) were seeded in complete medium in six-well plates. After 4 h of incubation, the medium was renewed with SPM in the presence or absence of 100 μ g/ml MG-BSA-AGEs for 24–72 h of incubation. Whole RNA extraction was performed using the RNeasy mini Kit (Qiagen Inc., Valencia, CA) in order to quantitatively monitor by real-time PCR the mRNA expression of human *Rage* (accession number AB036432) related to internal control house-keeping gene glyceraldehyde 3-phosphate dehydrogenase (GAPDH, accession number DQ403057). Complementary DNA (cDNA) was produced from total RNA extracts via reverse transcription using Transcripter first-strand cDNA synthesis kit (Roche Molecular Systems, Pleasanton, CA), and the reaction was carried out in Tetrad2 Thermal Cycler (Bio-Rad). The primer pair sequences used from Invitrogen (Life technologies, Paisley, UK) were: 5'-GGC TGG TGT TCC CAA TAA GG-3' and 3'-TCA CAG GTC

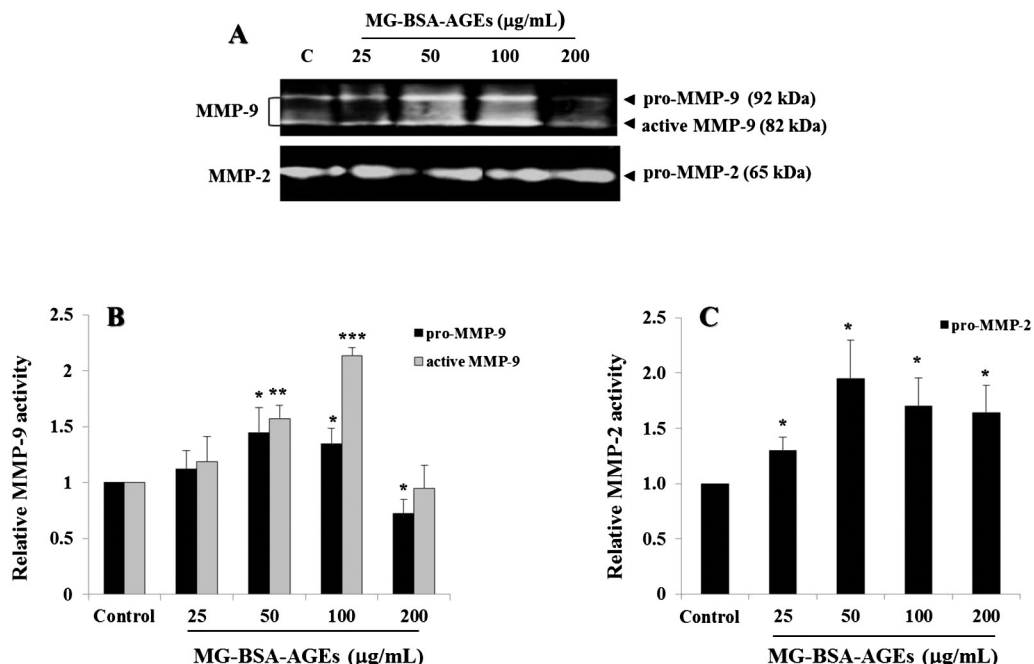
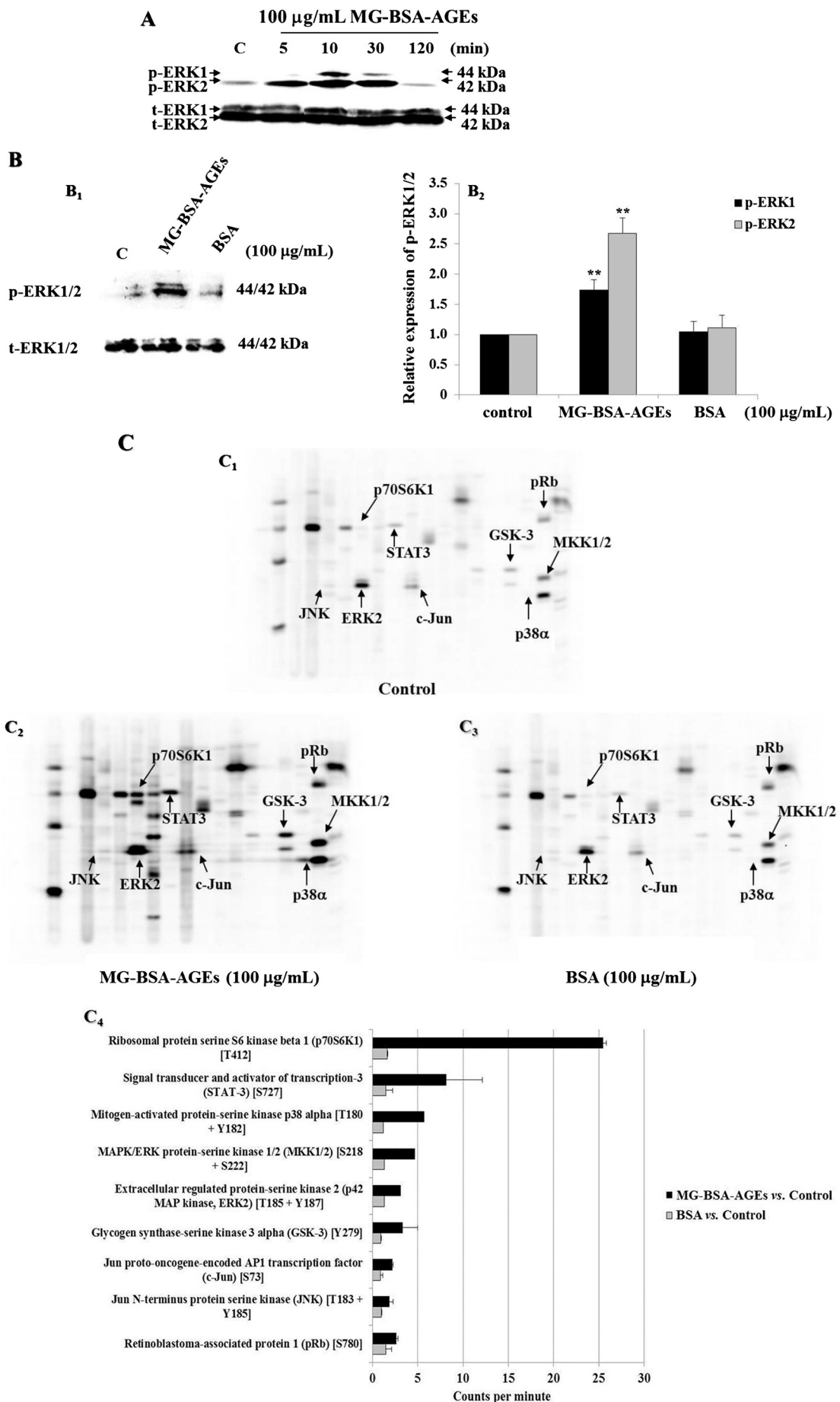


Fig. 4. Effect of MG-BSA-AGEs on MMP-9 and MMP-2 activities produced by breast cancer MDA-MB-231 cells during the Matrigel™ invasion assay. (A) Representative gelatin zymographic analysis showing the activity of MMP-9 and MMP-2 from cell conditioned media collected after Matrigel invasion assay by MDA-MB-231 cells treated with 25–100 μ g/ml MG-BSA-AGEs, compared with untreated cell-condition medium (control, c). The gels revealed gelatinolytic activities of pro- and active MMP-9 and pro-MMP-2. (B) Quantitative gelatinolytic activity of pro- and active MMP-9 and (C) pro-MMP-2 expressed as relative activity, which was calculated as a ratio of the control. Results are presented as mean \pm SD of four independent experiments. (*), (**), and (***) signify a statistically significant difference ($p < 0.05$, $p < 0.01$ and $p < 0.001$), compared with the control.



AGG GTT ACG GTT C-5' for human *Rage* as described previously [21] and 5'-TGA TGA CAT CAA GAA GGT GAA G-3' and 3'-TCC TTG GAG GCC ATG TGG GCC AT-5' for human GAPDH as designed using the primer3 software. The real-time PCR was performed using a QuantiTect Reverse Transcription kit containing PCR SyberGreen Master Mix (Applied Biosystems, Grand Island, NY) and performed on 7500 real-time PCR system (Applied Biosystems). For each analysis, a negative control was prepared using all the reagents except the cDNA template. All the reactions were run in triplicate, and the fold-change of expression was calculated according to delta delta Ct ($\Delta\Delta Ct$) method as follows: fold-change = $2^{(-\Delta\Delta Ct)}$ with $\Delta\Delta Ct = \Delta Ct$ ($RAGE_{treated} - GAPDH_{treated}$) – ΔCt ($RAGE_{control} - GAPDH_{control}$).

2.10. Flow cytometry analysis

MDA-MB-231 cells ($6 \times 10^5/2$ ml) were seeded in complete medium in six-well plates. After 48 h of incubation, the medium was renewed with SPM for a further 24-h incubation, and then 100 μ g/ml MG-BSA-AGEs or non-modified BSA were added for a 10-min incubation. Each condition was performed in triplicate. The cells were washed with PBS then scraped to maintain intact the structure of the transmembrane RAGE protein. After centrifugation (300g for 10 min), 10^6 cells were re-suspended in 20 μ l of PBS then 20 μ g/ml of mouse anti-RAGE (E-1) antibody or 2 μ g of mouse IgG1 isotype control (ab91353 from Abcam) were added. The mixture was then kept on ice for 45 min. The excess antibody was removed by washing the cells twice with PBS followed by centrifugation. After the second centrifugation, the cells were re-suspended in 20 μ l of PBS, and 20 μ g/ml of monoclonal anti-mouse antibody-FITC (Invitrogen, Paisley, UK) were added. The mixture was then kept on ice for 30 min. The RAGE expression level was measured using FACScan analysis software from FACSCalibur Flow Cytometer (Becton Dickinson).

2.11. Kinexus phospho-protein array analysis

MDA-MB-231 cells ($6 \times 10^5/2$ ml) were seeded in complete medium in six-well plates. After 48 h of incubation, the medium was changed to SPM. After a further 24-h incubation, 100 μ g/ml MG-BSA-AGEs or non-modified BSA were added, and the cells which were then incubated for 10 min at 37 °C. To determine the protein expression profile of signaling pathways downstream of RAGE, a phospho-protein array analysis (Kinetworks PhosphoSite Screen, KPSS-1.3) was performed by Kinexus Bioinformatics (Vancouver, Canada). Protein samples (500 μ g) from MG-BSA-AGE- or non-modified BSA-treated and untreated cells were extracted according to the manufacturer's instructions. The samples were used for a multi-immunoblotting assay based on SDS-polyacrylamide mini-gel electrophoresis with 20-lane multi-immunoblotters using different primary antibodies. Most of the multi-immunoblotting assays were performed at least twice. Protein expressions were visualized by chemiluminescence and relative expression was determined by Kinexus and expressed in counts per minute.

2.12. RAGE neutralization

To investigate whether MG-BSA-AGEs act through RAGE, the cells were treated with an anti-RAGE antibody to neutralize all the RAGE receptors. Briefly, MDA-MB-231 cells were seeded in complete medium

in 24-well plates according to the protocols of upstream applications previously described. The medium was renewed with SPM, and then 20 μ g/ml mouse monoclonal anti-RAGE [E-1] antibody or 20 μ g/ml IgG1, which was used as an isotype control, was added. After 1 h of incubation, the cells were treated with 100 μ g/ml MG-BSA-AGEs for 10 min or a 24–72-h stimulation at 37 °C followed by RNA or protein extraction for real-time RT-PCR and Western blotting. The cells were also eventually subjected to all functional cell-based assays mentioned previously. Each condition was performed in triplicate, and each experiment was repeated three times.

2.13. Statistical analysis

Results are expressed as the mean \pm standard deviation (SD). Experimental points were gathered for a minimum of three independent experiments. An unpaired Student's t-test was used for the comparison of two groups. A value of $P < 0.05$ was considered significant.

3. Results

3.1. MG-BSA-AGEs increase MDA-MB-231 cell proliferation

We first evaluated the effects of increasing concentrations of MG-BSA-AGEs and non-modified BSA varying between 25 μ g/ml and 200 μ g/ml on MDA-MB-231 cell proliferation (see Section 2). We found that MG-BSA-AGEs affected cell number, in a dose-dependent manner, increasing then decreasing cell proliferation as a bell-shaped curve. A peak of stimulation (2.0-fold increase, $p < 0.01$) was attained in the presence of 50 and 100 μ g/ml MG-BSA-AGEs, whereas the highest concentration (200 μ g/ml) did not alter the cell growth compared with the untreated cells used as control (Fig. 1A). To estimate the specific effect of MG-BSA-AGEs on cell proliferation, non-modified BSA was also tested. Compared with the control, only a low concentration of BSA (50 μ g/ml) slightly increased cell proliferation (1.25-fold, $p < 0.05$) whereas no effect was observed with other concentrations (Fig. 1A). Furthermore, for each condition, the percentage cell viability was assessed by trypan blue exclusion and revealed a high cell viability between 97% and 85% from the control to the highest concentration of MG-BSA-AGEs or non-modified BSA (Fig. 1B).

3.2. MG-BSA-AGEs increase MDA-MB-231 cell migration

To assess the effect of MG-BSA-AGEs on the migration of the breast cancer cell line MDA-MB-231, the cells were subjected to the wound-healing assay followed by a 24-h treatment in SPM (which reduced the cell growth) with different concentrations (25–200 μ g/ml) of MG-BSA-AGEs or non-modified BSA (Fig. 2). Representative photomicrographs of cell migration in untreated condition used as control (Fig. 2A), or treated conditions either with 50 μ g/ml MG-BSA-AGEs (Fig. 2B) or non-modified BSA (Fig. 2C) are shown. Compared with the control (Fig. 2A and D) and to non-modified BSA (Fig. 2C and D), MG-BSA-AGEs at concentrations of 25–100 μ g/ml increased the number of migrated cells (2.0-fold, $p < 0.05$, Fig. 2D). MG-BSA-AGEs significantly increased the distance of cell migration in a dose-dependent manner with a peak at 50 μ g/ml (2.0-fold increase, $p < 0.01$), compared with the control (Fig. 2D). No change in cell migration was observed with

Fig. 5. Effect of MG-BSA-AGEs on the phosphorylation of signaling proteins in MDA-MB-231 cells. (A) Representative Western blot analysis showing phosphorylation of ERK1/2 (p-ERK1/2) induced by 100 μ g/ml MG-BSA-AGEs after different incubation times varying from 5 to 120 min, compared with untreated cells (control). (B) Representative Western blot analysis (B_1) showing the effect of 100 μ g/ml MG-BSA-AGEs or non-modified BSA on the phosphorylation of ERK1/2 expression, compared with the control. (B_2) Relative phosphorylation of ERK1/2 calculated as a ratio to the total ERK1/2 (t-ERK1/2), the loading control. Results are presented as mean \pm SD of three independent experiments. (**) signifies a statistically significant difference ($p < 0.01$), compared with the control. (C) Multi-immunoblotting of 35 phospho-proteins expressed in untreated (C_1) MDA-MB-231 cells, cells treated with 100 μ g/ml MG-BSA-AGEs (C_2) or cells treated with non-modified BSA (C_3) after 10 min of incubation. (C_4) The bar graph shows the relative expression of the relevant phospho-proteins expressed in counts per minute and calculated as a ratio to the untreated cells (control).

the highest concentration of MG-BSA-AGEs (Fig. 2D). Although non-modified BSA had no effect on MDA-MB-231 cell migration at most concentrations, treatment with the highest concentration (200 µg/ml) resulted in a significant inhibition (40% decrease, $p < 0.05$) in the distance migrated as compared with the control (Fig. 2D).

3.3. MG-BSA-AGEs increase MDA-MB-231 cell invasion

The invasion of the basement membrane is a critical step during tumor progression because the basement membrane represents the last barrier for the cancer cells to reach the circulatory system and to be disseminated via metastasis. The effect of MG-BSA-AGEs on the MDA-MB-231 cell invasion was estimated by counting the stained migrated cells that passed across the porous membrane after invading the Matrigel™, a reconstituted basement membrane (Fig. 3). Representative photomicrographs of cell invasion in untreated condition considered as control (Fig. 3A) or treated either with MG-BSA-AGEs (Fig. 3B) or non-modified BSA (Figs. 3C) are shown. Compared with the control (Fig. 3A), MG-BSA-AGEs at 50 µg/ml and 100 µg/ml (Fig. 3C) significantly increased MDA-MB-231 cell invasion (2.0-fold, $p < 0.01$) (Fig. 3D). By contrast, MG-BSA-AGEs at 25 µg/ml and 200 µg/ml did not induce any significant changes in cell invasion, compared with the control. At all concentrations used, no effect of non-modified BSA on MDA-MB-231 cell invasion was observed, compared with the control (Fig. 3D).

3.4. MG-BSA-AGEs enhance MMP-9 activity

Matrix metalloproteinases (MMP)-2 and MMP-9, also called gelatinases, play a central role in the degradation of the type IV collagen of the basement membrane, thus contributing to tumor invasion and metastasis. Compared with the MMP-9 activity in untreated MDA-MB-231 cell-condition medium (control) as assessed by gelatine substrate zymography, treatment with 50 and 100 µg/ml MG-BSA-AGEs significantly ($p < 0.01$) enhanced MMP-9 activity (1.5-fold and 2.1-fold, respectively, Fig. 4A and B). A decrease in the activity of pro-MMP-9, which is the precursor and inactive form of MMP-9, was noticed when the cells were treated with 200 µg/ml MG-BSA-AGEs, compared with the control (Fig. 4A and B). The activity of pro-MMP-2 was enhanced after treatment with MG-BSA-AGEs at all concentrations used; however, no active MMP-2 was observed (Fig. 4).

3.5. MG-BSA-AGEs increase the phosphorylation of signaling proteins

To optimize incubation time corresponding to the maximal cell signaling induced by 100 µg/ml MG-BSA-AGEs (concentration previously shown to significantly increase all MDA-MB-231 cell functions), Western blotting was used to determine the expression levels of phospho-ERK1/2 (p-ERK1/2) in MDA-MB-231 cells treated with MG-BSA-AGEs for 5, 10, 30 and 120 min (Fig. 5). MG-BSA-AGEs increased the phosphorylation of ERK1/2 in cells after 5 min of incubation (Fig. 5). The maximum p-ERK1/2 expression level was reached at the 10-min incubation point. Expression levels of p-ERK1/2 slightly decreased after 30 min of incubation and nearly disappeared at 120-min incubation point (Fig. 5A). To confirm the effect of MG-BSA-AGEs on p-ERK1/2 expression level, MDA-MB-231 cells were treated with or without 100 µg/ml MG-BSA-AGEs or non-modified BSA for 10 min (Fig. 5B). Compared with untreated cells (control), MG-BSA-AGE treatment increased the phosphorylation of ERK1/2 (1.8- and 2.8-fold increase for p-ERK1 and p-ERK2, respectively) while no change of ERK1/2 phosphorylation was observed in non-modified BSA-treated cells (Fig. 5B).

A wider investigation of the downstream phosphorylated proteins of MG-BSA-AGEs/RAGE signaling pathways was proceeded as follows: the whole cell lysates of untreated MDA-MB-231 cells (control, Fig. 5C₁) or cells treated with 100 µg/ml MG-BSA-AGEs (Fig. 5C₂) and 100 µg/ml non-modified BSA (Fig. 5C₃) were analyzed using the phospho-protein array analysis KPSS-1.3 for 35 phospho-proteins including p-ERK2

(Fig. 5C). Like using Western blot analysis, quantification of the immuno-blots showed that MG-BSA-AGEs also resulted in a 3.0-fold increase of ERK2 phosphorylation, which reinforced the reproducibility and the validity of the data (Fig. 5B). MG-BSA-AGEs increased the phosphorylation of the ribosomal protein serine S6 kinase (p70S6K)-beta 1 (25.4-fold increase), the signal transducer and activator of transcription (STAT)-3 (8.0-fold increase), MAPK p38 and glycogene synthase-serine kinase (GSK)-3 α (5.6-fold and 3.2-fold, respectively), and MAPK/ERK protein-serine kinase 1/2 (MKK1/2, 4.6-fold increase), compared with untreated cells (Fig. 5C₄). Furthermore, the phosphorylation of c-Jun and its kinase JNK was increased (2.0-fold) in MG-BSA-AGE-treated cells as compared with untreated cells (control). The phosphorylation of the tumor-suppressor protein retinoblastoma-associated protein-1 (pRb) was also increased (2.6-fold) in MG-BSA-AGE-treated cells. Cell treatment with 100 µg/ml non-modified BSA had no significant effects on the phosphorylation of the proteins studied, compared with the control (Fig. 5C).

3.6. MG-BSA-AGEs up-regulate RAGE expression

A time-course of expression levels of RAGE in MDA-MB-231 cells following treatment with 100 µg/ml MG-BSA-AGEs was established using Western blotting and real-time RT-PCR. MG-BSA-AGEs treatment led to up-regulation of RAGE protein levels in a time-dependent manner (Fig. 6A). Within 10 min, RAGE expression levels increased in MG-BSA-AGE-treated cells, compared with the basal level of RAGE expressed in untreated cells (Fig. 6A). These data were further confirmed using flow cytometry analysis (Fig. 6B). Western blot analysis revealed a peak of RAGE protein expression levels (3.0-fold increase, $p < 0.0001$) after 24 h of incubation with MG-BSA-AGEs, whereas a peak of RAGE mRNA expression (5.0-fold increase, $p < 0.001$) was noticed after 48 h of incubation (Fig. 6C). After 72 h of incubation with MG-BSA-AGEs, there was not significant difference in RAGE transcript and protein levels between MG-BSA-AGEs treated and untreated cells (Fig. 6).

3.7. MG-BSA-AGEs stimulate MDA-MB-231 cells through RAGE

To check whether MG-BSA-AGEs stimulated MDA-MB-231 cells through their major receptor RAGE, the cells were pre-treated with either a neutralizing RAGE antibody to block all the RAGE receptors or with an isotype control IgG1 used as a negative control (Fig. 7). RAGE neutralization process was applied to verify whether MG-BSA-AGEs induce the increased phosphorylation of signaling proteins such as ERK1/2 (the key protein of signaling pathways) and p70S6K1 (the most over-phosphorylated protein induced by MG-BSA-AGEs) through RAGE. The isotype control IgG1 did not affect ERK1/2 phosphorylation induced by MG-BSA-AGEs, compared with the basal expression level of p-ERK1/2 in untreated cells used as control (Fig. 7A). However, 100 µg/ml BSA-AGEs did not enhance ERK1/2 phosphorylation in the cells pre-treated with neutralizing RAGE antibody (Fig. 7A). In addition, the protein array analysis previously described was confirmed by a similar concomitant increase of p70S6K1 phosphorylation induced by MG-BSA-AGEs even in IgG1-treated cells, compared with the control (Fig. 7B). The blockade of RAGE completely inhibited MG-BSA-AGE-induced p70S6K1 phosphorylation (Fig. 7B). On the cell function aspects, the addition of MG-BSA-AGEs to IgG1-pretreated cells induced a significant increase in cell proliferation (1.8-fold, $p < 0.001$, Fig. 7C), cell migration (2.0-fold, $p < 0.05$, Fig. 7D) and cell invasion (1.6-fold, $p < 0.05$, Fig. 7E) as compared with the untreated cells (control). However, the addition of MG-BSA-AGEs to cells pre-treated with anti-RAGE antibody did not change the cellular processes as compared with the control. Altogether, MG-BSA-AGEs lost their biological effects after the blockade of RAGE, demonstrating that MG-BSA-AGEs act through RAGE.

4. Discussion

Diabetes and cancer are a cause for concern because of the high incidence of these diseases in Western countries and, more recently, in

developing countries. A growing body of epidemiological evidence suggests a molecular link between diabetes and breast cancer [31,32]. In diabetic patients, the most circulating and abundant advanced glycation endproducts (AGEs)-derived protein is serum glycated albumin [33].

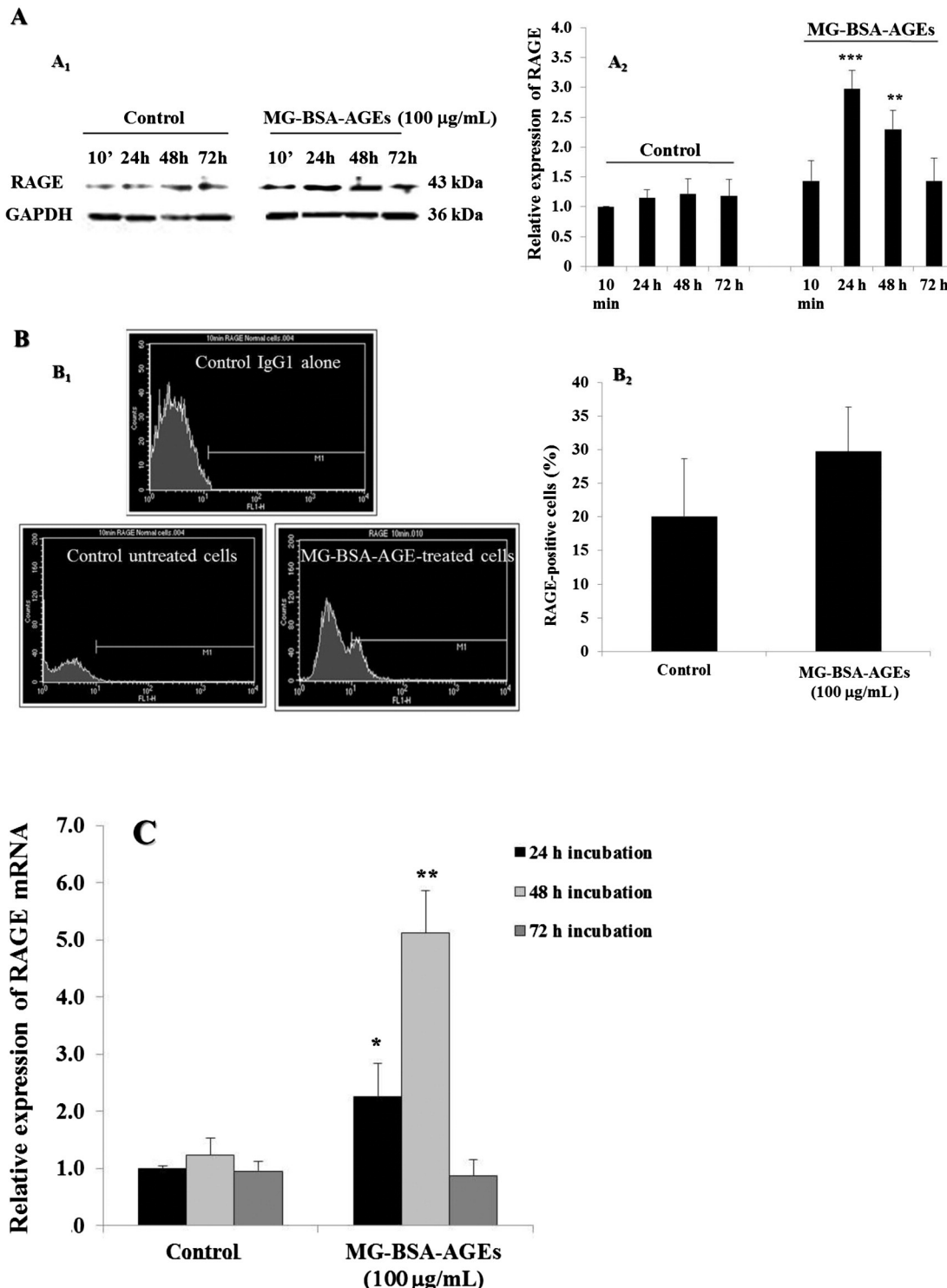


Fig. 6. Time-course of RAGE protein and mRNA expression in breast cancer MDA-MB-231 cells treated with MG-BSA-AGEs. (A) Representative Western blot analysis (A₁) showing the effect of 100 µg/ml MG-BSA-AGEs on RAGE expression in MDA-MB-231 cells after incubation for 10 min or 24, 48 or 72 h, compared with untreated cells (control). Bar graph (A₂) showing the relative expression of RAGE calculated as a ratio to GAPDH expression, the loading control. (B) Representative FACS analysis (B₁) of the RAGE up-regulation induced by 100 µg/ml MG-BSA-AGEs after 10 min of incubation. IgG1 was used as an isotype control. Bar graph (B₂) indicating the quantification of the percentage of RAGE-positive cells calculated as a ratio to isotype control. (C) Relative expression of RAGE mRNA as determined using real-time PCR analysis. Results are presented as mean ± SD of three independent experiments. (*) and (**) signify a statistically significant difference ($p < 0.05$ and $p < 0.01$), compared with the control.

In patients with breast cancer, serum concentrations of AGEs were higher than in healthy controls [32]. To date, the biological effects of glycated albumin on human breast cancer cells have been poorly described.

Here, we have shown that MG-BSA-derived AGEs increase the proliferation, migration and invasion (associated with an enhancement of MMP-9 gelatinase activity) of the invasive and non-hormone-dependent cell line MDA-MB-231 *in vitro*. Furthermore, MG-BSA-AGEs increase expression of RAGE and phosphorylation of ERK1/2 and other key signaling proteins such as p70S6K1. In addition, the blockade of RAGE using a neutralizing RAGE antibody removes all these MG-BSA-AGE effects. By contrast, non-modified BSA showed little biological effects on MDA-MB-231 cells. These new findings suggest that AGEs might contribute to the development and progression of invasive breast

cancer. RAGE over-expression and the phosphorylation of key proteins induced by AGEs might represent promising targets for drug therapy to treat diabetic patients with breast cancer.

MG-BSA-AGEs increased MDA-MB-231 cell proliferation, migration and invasion, in a dose-dependent manner as shown by a bell-shaped curve, while non-modified BSA had no biological effects, except a slight stimulatory effect on cell proliferation at 50 µg/ml and an inhibitory effect on cell migration at 200 µg/ml. This slight pro-mitogenic effect of non-modified BSA is correlated with the induction of ERK1/2 phosphorylation observed at short incubation time (10 min) at the same concentration (50 µg/ml) in our pilot studies (data not shown), whereas no increase in phosphorylation of ERK1/2 was induced by 100 µg/ml of non-modified BSA. The pro-mitogenic effect of native BSA was also reported by Chung and colleagues using tubular epithelial cells in similar

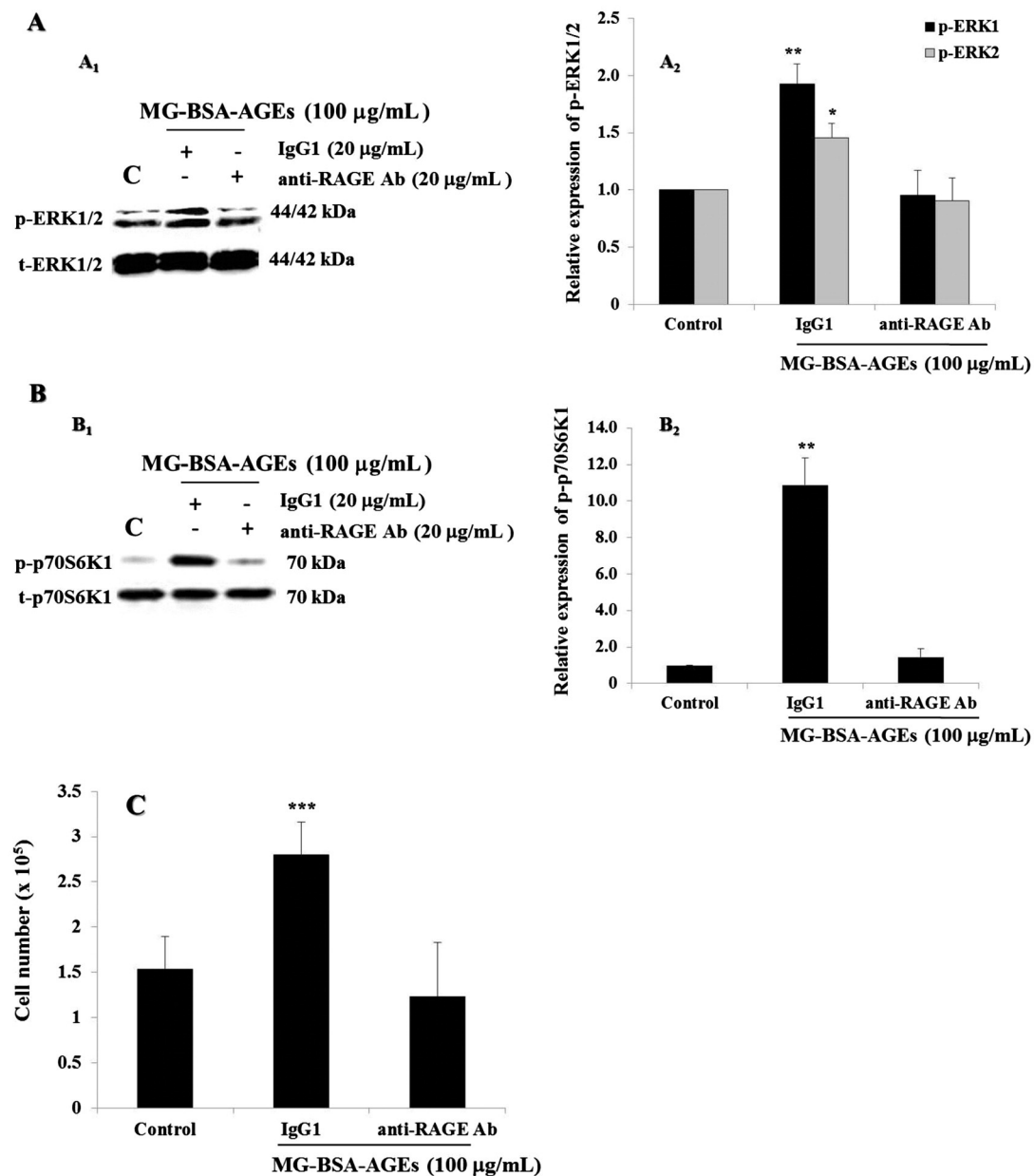


Fig. 7. RAGE mediates the effects of MG-BSA-AGEs in breast cancer MDA-MB-231 cells. Representative Western blot analysis showing the loss of MG-BSA-AGE-induced phosphorylation of (A) ERK1/2 and (B) p70S6K1 after the blockade of RAGE by an anti-RAGE antibody, compared with untreated cells (control) and an isotype control IgG1. Bar graphs show the relative expression levels of (A₂) p-ERK1/2 and (B₂) p-p70S6K1 calculated as a ratio to the total ERK1/2 (t-ERK1/2) and total p70S6K1 (t-p70S6K1), the respective loading controls. Loss of MG-BSA-AGE-induced (C) cell proliferation, (D) migration and (E) invasion after RAGE blockade using a neutralizing blocking anti-RAGE antibody, compared with untreated cells (control) and an isotype control IgG1. Results are presented as mean \pm SD of three independent experiments. (*) and (**) signify a statistically significant difference ($p < 0.05$ and $p < 0.01$), compared with the control.

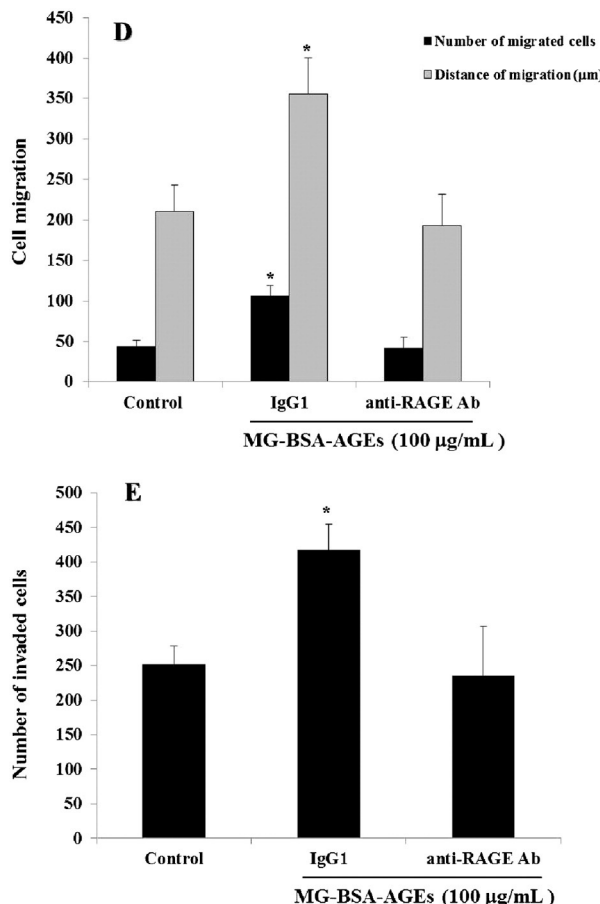


Fig. 7 (continued).

conditions [34]. This slight positive effect might be attributed to a traceable amount of AGEs reported to be observed in native albumin, the most common serum protein known to be readily glycated *in vivo*. Indeed, native albumin is modified by 0.3 mol/mol of sugars and this is likely to be by glucose, the major metabolic sugar [35]. However, modification by other sugars such as methylglyoxal cannot be ruled out and may contribute towards AGE formation on native albumin. In contrast, the inhibitory effect of high concentration of native BSA on cell migration may be caused by the inhibition of cell adhesion, which plays a critical role in cell motility, due to the high adsorption of BSA between the culture medium and the solid surface as it was previously reported [36]. Here, bell-shaped curves representing the MDA-MB-231 cell response to MG-BSA-AGE biological effects are indicative of a bivalent bridging mechanism describing the dimerization/oligomerization of specific cell-surface receptors after binding with the ligand [37]. Indeed, throughout this present study, the maximal cell response was obtained with 50 and 100 µg/ml MG-BSA-AGEs, which might correspond to the optimal oligomerization of the AGE receptor such as RAGE to induce the maximal signaling. Therefore, the loss of the cell response seen at the highest concentration (i.e. 200 µg/ml) of MG-BSA-AGEs may be due to impediment of RAGE oligomerization. Furthermore, using an epitope-defined monoclonal antibody that specifically recognizes receptor oligomerization, Xu and colleagues demonstrated the importance of RAGE oligomerization for the formation of active signaling complexes [38]. In addition, a recent study provides insights into the factors that influence AGEs–RAGE binding including glycation agent like methylglyoxal and the RAGE structure [39]. Indurthi et al. [39] used 1 and 5 mM methylglyoxal to modify BSA respectively; they demonstrated that higher concentration of methylglyoxal produced more AGEs, which showed increased binding affinity to RAGE. They suggested that

higher glycation generate more potential binding sites for RAGE in the protein surface [39]. In the present study, we applied 100 mM methylglyoxal to generate MG-BSA-AGEs to ensure a high binding potential to RAGE. Using siRNA technology, RAGE has been shown to play a critical role in the growth of human breast cancer cell lines, including MDA-MB-231 [21]. Most studies on BSA-AGEs, including this investigation, compare the biological effects of MG-BSA-AGEs with native non-modified BSA, which in agreement with previous work show no biological effects or little effects at the concentrations or experimental conditions used [40]. Indeed, native globular BSA even bound to the cell surface rarely triggers specific transduction signaling unlike BSA-AGEs [41,42]. Therefore, the mode of action of MG-BSA-AGEs is dependent on pathways mediated via RAGE rather than BSA-mediated pathways.

In this present study, we also showed that the enhancement of MDA-MB-231 cell invasive capacity induced by MG-BSA-AGEs was associated with MMP-9 gelatinase activity without changing MMP-2 gelatinase activity. Non-modified BSA had no effect on both MMP activities. Invasion and metastasis are key cell events resulting in tumor progression and are the hallmarks of cancer malignancy. During metastasis, cancer cells degrade the matrix by production and secretion of MMPs. MMPs facilitate cell migration and invasion across the connective tissue and the basement membrane to reach the blood circulation which is the main route of tumor dissemination towards vascularized organs. A study has shown that incubating human lung adenocarcinoma cell with glyceraldehyde-AGEs for 48 h, promoted cell migration and invasion across Matrigel™ with enhancement of MMP-2 activity but not MMP-2 mRNA [43]. Recently, Noh and colleagues reported MMP-2 from body fluid as a putative biomarker in metastatic breast cancer [44]. However, Hallett and colleagues targeted MMP-9 mRNA in a mouse model using anti-MMP-9 DNAzyme transfected into MDA-MB-231 cells, and they reported a decrease of breast cancer and confirmed the key role of MMP-9 in breast cancer metastasis [45]. Furthermore, using a murine macrophage cell line, it has been shown that AGEs have regulated MMP-9 production via RAGE, which is in agreement with our present work, and was associated with activation of ERK1/2, p38 MAPK and NF-κB [46]. Therefore, our results suggest that MG-BSA-AGEs might promote breast tumor progression by increasing cancer cell migration, invasion and MMP-9 activity.

During MDA-MB-231 cell treatment with MG-BSA-AGEs, the cells displayed a maximum RAGE up-regulation after 24 h of incubation. Recently, Shi and colleagues reported that AGEs up-regulate RAGE expression in various tissues, reaching a maximum after a 24-h treatment, which facilitates the AGE–RAGE response by forming a positive feedback loop [41]. This suggests that RAGE up-regulation induced by MG-BSA-AGEs may contribute to the increased cellular response assessed as proliferation, migration and invasion. In addition, in endothelial progenitor cells, BSA-AGE-induced RAGE up-regulation has been demonstrated to be ERK1/2 and p38 MAPK-dependent but not mediated by JNK MAPK [47]. We observed the peak up-regulation of RAGE mRNA expression level after 48 h of treatment with MG-BSA-AGEs, whereas the protein expression level was lower, indicating a negative-feedback loop of the translational regulatory system of RAGE protein expression. To confirm this hypothesis, additional studies might be of interest on the key factors regulating the translational system of RAGE protein expression such as, microRNA and nuclear transcription factors p65/50 NF-κB and Sp-1/ERα, previously demonstrated to be involved in this regulatory process [48].

p-ERK1/2 is a phospho-protein widely known to play a central role in most cellular responses including cell proliferation, migration and invasion. We found that the optimal signal for MG-BSA-AGE-induced p-ERK1/2 expression in MDA-MB-231 cell line was obtained after 10-min treatment. Similar early phosphorylation of ERK1/2 was reported to be induced by BSA-AGEs in various cell types [34]. We demonstrated that MG-BSA-AGEs enhanced phosphorylation of ERK1/2 and stimulated all cellular functions through RAGE, as these processes were attenuated after neutralization of the receptor using a specific monoclonal

antibody. Thus, this result eliminates the involvement of other AGE receptors such as CD36, scavenger receptors class A type II, class B type I and AGE receptors 1, 2 and 3, which are mainly implicated in the detoxification of AGEs rather than in signaling processes [49].

Although 100 µg/ml non-modified BSA did not change the phosphoproteome profile of MDA-MB-231 cells compared to untreated cells, at a similar concentration, MG-BSA-AGEs concomitantly increased the phosphorylation of p70S6K1, STAT-3, p38 MAPK, GSK-3 and MKK1/2. The p70S6K1 has been demonstrated to play a central role in tumor growth by regulating pro-angiogenic effects and protein synthesis of insulin [50,51]. In addition, targeting p70S6K1 gene expression by micro-RNA 145 expression has been reported to inhibit tumor growth [52]. Constitutively active STAT proteins, which are critical in the regulation of cell cycle and cell growth, are found in various types of tumors including breast cancer [53]. Previous studies have reported p38 MAPK as a central kinase in a common intracellular signaling pathway that plays an essential role in human breast cancer cell migration and invasion by modulating the expression and activity of MMPs [54]. Furthermore, several lines of evidences suggest a link between p38 MAPK activation and MMP-9 expression [55]. In some reports, the use of pharmacological inhibitors of GSK-3 and of p38 MAPK, which are proteins with increased phosphorylation observed in our study, in MDA-MB-231 cells and in a model mouse of breast cancer demonstrated the key requirement of these proteins in breast cancer development [56,57]. Here, we also showed that MG-BSA-AGE-induced p70S6K1 overphosphorylation was prevented after RAGE neutralization, which further removes all the biological effects of MG-BSA-AGEs-induced MDA-MB-231 cell proliferation, migration and invasion. Thus, altogether, targeting either the expression of phospho-proteins aforementioned such as p70S6K1 or targeting RAGE expression might prevent the progression and development of breast cancer in diabetic patients.

In conclusion, as a consequence of BSA glycation, this study demonstrated the stimulatory effects of MG-BSA-AGEs on cell proliferation, migration and invasion (with an enhancement of MMP-9 activity) through RAGE, in an invasive and non-hormone-dependent breast cancer cell line MDA-MB-231. Among the phospho-proteins involved in MG-BSA-AGE-induced signaling pathways, we also highlighted a concomitant increase in the phosphorylation of p70S6K1, which might be a new biomarker of the invasive subtype of the breast cancer and a promising target drug like RAGE to fight against breast cancer in diabetic patients.

Acknowledgments

We are grateful to the Ministry of Health, Saudi Arabia for providing a PhD scholarship to Hana Sharaf that enabled her to undertake this study. We would like to thank Dr Nasser Al-Shanti, School of Healthcare Science at Manchester Metropolitan University for his help with flow cytometry analysis and Tor Yip for his assistance with the illustrations.

References

- [1] L.J. Sparvero, D. Asafu-Adjei, R. Kang, D. Tang, N. Amin, J. Im, R. Rutledge, B. Lin, A.A. Amoscato, H.J. Zeh, M.T. Lotze, RAGE (receptor for advanced glycation endproducts), RAGE ligands, and their role in cancer and inflammation, *J. Transl. Med.* 7 (2009) 17.
- [2] L.C. Maillard, Action des acides aminés sur les sucres: formation des mélanoïdines par voie méthodique, *C. R. Acad. Sci.* 154 (1912) 66–68.
- [3] N. Ahmed, Advanced glycation endproducts-role in pathology of diabetic complications, *Diabetes Res. Clin. Pract.* 67 (2005) 3–21.
- [4] A. Elostá, T. Ghous, N. Ahmed, Natural products as anti-glycation agents: possible therapeutic potential for diabetic complications, *Curr. Diabetes Rev.* 8 (2012) 92–108.
- [5] A.D. McCarthy, A.M. Cortizo, G. Giménez-Segura, L. Bruzzone, S.B. Etcheverry, Non-enzymatic glycosylation of alkaline phosphatase alters its biological properties, *Mol. Cell. Biochem.* 181 (1998) 63–69.
- [6] M. Heilman, A. Wellner, G. Gadermaier, A. Ilchmann, P. Briza, M. Krause, R. Nagai, S. Burgdorf, S. Scheurer, S. Vieths, T. Henle, M. Toda, Ovalbumin modified with pyralline, a Maillard reaction product, shows enhanced T-cell immunogenicity, *J. Biol. Chem.* 289 (2014) 7919–7928.
- [7] I. Giardino, D. Edelstein, M. Brownlee, Non-enzymatic glycosylation *in vitro* and in bovine endothelial cells alters basic fibroblast growth factor activity: a model for intracellular glycosylation in diabetes, *J. Clin. Invest.* 94 (1994) 110–117.
- [8] G.K. Reddy, Cross-linking in collagen by nonenzymatic glycosylation increases the matrix stiffness in rabbit Achilles tendon, *Exp. Diabesity Res.* 5 (2004) 143–153.
- [9] S. Poggioli, H. Bakala, B. Friguet, Age-related increase of protein glycation in peripheral blood lymphocyte is restricted to preferential target proteins, *Exp. Gerontol.* 37 (2002) 1207–1215.
- [10] B.K. Kilhord, T.J. Berg, K.I. Birkeland, P. Thorsby, K.F. Hanssen, Serum levels of advanced glycation endproducts are increased in patients with type 2 diabetes and coronary heart disease, *Diabetes Care* 22 (1999) 1543–1548.
- [11] V.V. Shuvaev, I. Laffont, J.M. Serot, J. Fujii, N. Taniguchi, G. Siest, Increased protein glycation in cerebrospinal fluid of Alzheimer's disease, *Neurobiol. Aging* 22 (2001) 397–402.
- [12] E. Sato, F. Mori, S. Igarashi, T. Abiko, M. Takeda, S. Ishiko, A. Yoshida, Corneal advanced glycation endproducts increase with proliferative diabetic retinopathy, *Diabetes Care* 24 (2001) 479–482.
- [13] B.A. Perkins, N. Rabban, A. Weston, L.H. Ficociello, A. Adaikalakoteswari, M. Niewczas, J. Warram, A.S. Krolewski, P. Thornally, Serum levels of advanced glycation endproducts and other markers of protein damage in early diabetic nephropathy in type 1 diabetes, *PLoS ONE* 7 (2012) e356551.
- [14] R. Abe, T. Shimizu, H. Sugawara, H. Watanabe, H. Nakamura, H. Choei, N. Sasaki, S. Yamagishi, M. Takeuchi, H. Shimizu, Regulation of human melanoma growth and metastasis by AGE-AGE receptor interactions, *J. Invest. Dermatol.* 122 (2004) 461–467.
- [15] S. Gangemi, A. Allegra, M. Aguennouz, A. Alonci, A. Speciale, A. Cannavo, M. Cristani, S. Russo, G. Spatari, A. Alibrandi, C. Musolino, Relationship between advanced oxidation protein products, advanced glycation endproducts, and S-nitrosylated proteins with biological risk and MDR-1 polymorphisms in patients affected by B-chronic lymphocytic leukemia, *Cancer Investig.* 30 (2012) 20–26.
- [16] R. López-Díez, A. Rastrojo, O. Villate, B. Aguado, Complex tissue-specific patterns and distribution of multiple RAGE splice variants in different mammals, *Genome Biol. Evol.* 5 (2013) 2420–2435.
- [17] T. Shimomoto, Y. Luo, H. Ohmori, Y. Chihara, K. Fujii, T. Sasahira, A. Denda, H. Kuniyasu, Advanced glycation endproducts (AGE) induce the receptor for AGE in the colonic mucosa of azoxymethane-injected Fischer 344 rats fed with a high-linoleic acid and high-glucose diet, *J. Gastroenterol.* 47 (2012) 1073–1083.
- [18] P. Pichíule, J.C. Chavez, A.M. Schmidt, S.J. Vannucci, Hypoxia-inducible factor-1 mediates neuronal expression of the receptor for advanced glycation endproducts following hypoxia/ischemia, *J. Biol. Chem.* 282 (2007) 36330–36340.
- [19] E.M. Akirav, P. Preston-Hurlburt, J. Garyu, O. Henegariu, R. Clynes, A.M. Schmidt, K.C. Herold, RAGE expression in human T cells: a line between environmental factors and adaptative immune responses, *PLoS ONE* 7 (2012) e34698.
- [20] Y. Li, S. Liu, Z. Zhang, Q. Xu, F. Xie, J. Wang, S. Ping, C. Li, Z. Wang, M. Zhang, J. Huang, D. Chen, L. Hu, C. Li, RAGE mediates accelerated diabetic vein graft atherosclerosis induced by combined mechanical stress and AGEs via synergic ERK activation, *PLoS ONE* 7 (2012) e35016.
- [21] A.M. Radia, A.M. Yaser, X. Ma, J. Zhang, C. Yang, Q. Dong, P. Rong, B. Ye, S. Liu, W. Wang, Specific siRNA targeting receptor for advanced glycation endproducts (RAGE) decreases proliferation in human breast cancer cell lines, *Int. J. Mol. Sci.* 14 (2013) 7959–7978.
- [22] J. Xie, J.D. Méndez, V. Méndez-Valenzuela, M.M. Aguilar-Hernández, Cellular signaling of the receptor for advanced glycation endproducts (RAGE), *Cell. Signal.* 25 (2013) 2185–2197.
- [23] Y.W. Yoon, T.S. Kang, B.K. Lee, W. Chang, K.C. Huang, J.H. Rhee, P.K. Min, B.K. Hong, S.J. Rim, H.M. Kwon, Pathobiological role of advanced glycation endproducts via mitogen-activated protein kinase dependent pathway in the diabetic vasculopathy, *Exp. Mol. Med.* 40 (2008) 398–406.
- [24] C. Liu, J.C. He, W. Cai, H. Liu, L. Zhu, H. Vlassara, Advanced glycation endproduct (AGE) receptor 1 is a negative regulator of the inflammatory response to AGE in mesangial cells, *Proc. Natl. Acad. Sci. U. S. A.* 101 (2004) 11767–11772.
- [25] J.S. Huang, J.Y. Guh, H.C. Chen, W.C. Hung, Y.H. Lai, L.Y. Chuang, Role of advanced glycation endproduct (RAGE) and the JAK/STAT-signaling pathway in AGE-induced collagen production in NRK-49 F cells, *J. Cell. Biochem.* 81 (2001) 102–113.
- [26] E.L. Guimaraes, C. Empsen, A. Geerts, L.A. van Grunsven, Advanced glycation endproducts induce production of reactive oxygen species via the activation of NADPH oxidase in murine hepatic stellate cells, *J. Hepatol.* 52 (2010) 389–397.
- [27] J.Y. Kim, H.K. Park, J.S. Yoon, S.J. Kim, E.S. Kim, K.S. Ahn, D.S. Kim, S.S. Yoon, B.K. Kim, Y.Y. Lee, Advanced glycation endproduct (AGE)-induced proliferation of HEL cells via receptor for AGE-related signal pathways, *Int. J. Oncol.* 33 (2008) 493–501.
- [28] G. Klein, E. Vellenga, M.W. Fraaije, W.A. Kamps, E.S.J.M. de Bont, The possible role of matrix metalloproteinase (MMP)-2 and MMP-9 in cancer, e.g. acute leukemia, *Crit. Rev. Oncol. Hematol.* 50 (2004) 87–100.
- [29] A. Riehl, J. Németh, P. Angel, J. Hess, The receptor RAGE: bridging inflammation and cancer, *Cell Commun. Signal.* 7 (2009) 12.
- [30] S. Liao, W. Wel, L. Wang, Y. Zhang, J. Li, C. Wang, S. Sun, Association between diabetes mellitus and breast cancer risk: a meta-analysis of the literature, *Asian Pac. J. Cancer Prev.* 12 (2011) 1061–1065.
- [31] A.M. Korwar, H.S. Bhonsle, A.D. Chougale, S.S. Kote, K.R. Gawai, V.S. Ghole, C.B. Koppikar, M.J. Kulkarni, Analysis of AGE modified proteins and RAGE expression in HER2/neu negative invasive ductal carcinoma, *Biochem. Biophys. Res. Commun.* 19 (2012) 490–494.
- [32] P. Tesarová, M. Kalousová, M. Jáchymová, O. Mestek, L. Petruzelka, T. Zima, Receptor for advanced glycation endproducts (RAGE)—soluble form (sRAGE) and gene polymorphisms in patients with breast cancer, *Cancer Investig.* 25 (2007) 720–725.

[33] N. Furusyo, J. Hayashi, Glycated albumin and diabetes mellitus, *Biochim. Biophys. Acta* 1830 (2013) 5509–5514.

[34] A.C. Chung, H. Zhang, Y.Z. Kong, J.J. Tan, X.R. Huang, J.B. Kopp, H.Y. Lan, Advanced glycation endproducts induce tubular CTGF via TGF β -independent Smad3 signaling, *J. Am. Soc. Nephrol.* 21 (2010) 249–260.

[35] N. Ahmed, A.J. Furth, A microassay for protein glycation based on the periodate method, *Anal. Biochem.* 192 (1991) 109–111.

[36] A. Carre, V. Lacarrriere, in: K.L. Mittal (Ed.), *Contact Angle, Wettability and Adhesion*, 5, VSP/Brill, Leiden, 2008, pp. 253–267.

[37] R.G. Posner, J. Bold, Y. Bernstein, J. Raso, J. Braslow, W.S. Hlavacek, A.S. Perelson, Measurement of receptor crosslinking at the cell surface via multiparameter flow cytometry, *Proc. SPIE* 3256, Advances in Optical Biophysics, 3256, 1998, pp. 132–143.

[38] D. Xu, J.H. Young, J.M. Krahin, D. Song, K.D. Corbett, W.J. Chazin, L.C. Pedersen, J.D. Esko, Stable RAGE-heparan sulfate complexes are essential for signal transduction, *ACS Chem. Biol.* 8 (2013) 1611–1620.

[39] V.S. Indurthi, E. Leclerc, S.W. Vetter, Interaction between glycated serum albumin and AGE-receptors depends on structural changes and the glycation reagent, *Arch. Biochem. Biophys.* 528 (2012) 185–196.

[40] L. Yu, Y. Zhao, S. Xu, F. Ding, C. Jin, G. Fu, S. Weng, Advanced glycation endproduct (AGE) – AGE receptor (RAGE) system upregulated connexin43 expression in rat cardiomyocytes via PKC and Erk MAPK pathways, *Int. J. Mol. Sci.* 14 (2013) 2242–2257.

[41] Z. Rasheed, N. Aktar, T.M. Haqqi, Advanced glycation endproducts induce the expression of interleukin-6 and interleukin-8 by receptor for advanced glycation endproduct-mediated activation of mitogen activated protein kinases and nuclear factor- κ B in human osteoarthritis chondrocytes, *Rheumatology* 50 (2011) 838–851.

[42] L. Shi, X. Yu, H. Yang, X. Wu, Advanced glycation endproducts induce human corneal epithelial cells apoptosis through generation of reactive oxygen species and activation of JNK and P38 MAPK, *PLoS ONE* 8 (2013) e66781.

[43] J. Takino, S. Yamagishi, M. Takeuchi, Cancer malignancy is enhanced by glyceraldehyde-derived advanced glycation endproducts, *J. Oncol.* 2010 (2010) 739852.

[44] S. Noh, J.J. Jung, M. Jung, K.H. Kim, H.Y. Lee, B. Wang, J. Cho, T.S. Kim, H.C. Jeung, S.Y. Rha, Body fluid MMP-2 as a putative biomarker in metastatic breast cancer, *Oncol. Lett.* 3 (2012) 699–703.

[45] M.A. Hallett, B. Teng, H. Hasegawa, L.P. Schwab, T.N. Seagroves, T. Pourmotabbed, Anti-matrix metalloproteinase-9 DNAzyme decreases tumor growth in the MMTV-PyMT mouse model of breast cancer, *Breast Cancer Res.* 15 (2013) R12.

[46] F. Zhang, G. Bunker, X. Liu, P.A. Suwanabol, J. Lengfeld, D. Yamanouchi, K.C. Kent, B. Liu, The novel function of advanced glycation endproducts in regulation of MMP-9 production, *J. Surg. Res.* 171 (2011) 871–876.

[47] C. Sun, C. Liang, Y. Ren, Y. Zhen, Z. He, H. Wang, H. Tan, X. Pan, Z. Wu, Advanced glycation endproducts depress function of endothelial progenitor cells via p38 and ERK1/2 mitogen-activated protein kinase pathways, *Basic Res. Cardiol.* 104 (2009) 42–49.

[48] N. Tanaka, H. Yonekura, S. Yamagishi, H. Fujimori, Y. Yamamoto, H. Yamamoto, The receptor for advanced glycation end products is induced by the glycation products themselves and tumor necrosis factor- α through nuclear factor- κ B, and by 17 beta-estradiol through Sp-1 in human vascular endothelial cells, *J. Biol. Chem.* 275 (2000) 25781–25790.

[49] G. Marsche, B. Weigle, W. Sattler, E. Malle, Soluble RAGE blocks scavenger receptor CD36-mediated uptake of hypochlorite-modified low-density lipoprotein, *FASEB J.* 21 (2007) 3075–3082.

[50] Q. Zhou, L.Z. Liu, X. Hu, X. Shi, J. Fang, B.H. Jiang, Reactive oxygen species regulate insulin-induced VEGF and HIF-1 alpha expression through activation of p70S6K1 in human prostate cancer cells, *Carcinogenesis* 28 (2007) 28–37.

[51] M.D. Dennis, L.S. Jefferson, S.R. Kimball, Role of p70S6K1-mediated phosphorylation of eIF4B and PDCD4 proteins in the regulation of synthesis, *J. Biol. Chem.* 287 (2012) 42890–42899.

[52] Q. Xu, L.Z. Liu, X. Qian, Q. Chen, Y. Jiang, D. Li, L. Lai, B.H. Jiang, MiR-145 directly targets p70S6K1 in cancer cells to inhibit tumor growth and angiogenesis, *Nucleic Acids Res.* 40 (2012) 761–774.

[53] S.S. Chung, C. Aroh, J.V. Vadgama, Constitutive activation of STAT3 signaling regulates hTERT and promotes stem cell-like traits in human breast cancer cells, *PLoS ONE* 8 (2013) e83971.

[54] X.F. Wang, Q.M. Zhou, J. Du, H. Zhang, Y.Y. Lu, S.B. Su, Baicalin suppresses migration, invasion and metastasis of breast cancer via p38 MAPK signaling pathway, *Anticancer Agents Med Chem.* 13 (2013) 923–931.

[55] H.R. Ranaivo, J.N. Hodge, N. Choi, M.S. Wainwright, Albumin induces upregulation of matrix metalloproteinase-9 in astrocytes via MAPK and reactive oxygen species-dependent pathways, *J. Neuroinflammation* 9 (2012) 68.

[56] H.M. Kim, C.S. Kim, J.H. Lee, S.J. Jang, J.J. Hwang, S. Ro, J. Choi, CG0009, a novel glycogen synthase kinase 3 inhibitor, induces cell death through cyclin D1 depletion in breast cancer cells, *PLoS ONE* 8 (2013) e60383.

[57] D. Sukhtankar, A. Okun, A. Chandramouli, M.A. Nelson, T.W. Vanderah, A.E. Cress, F. Porreca, T. King, Inhibition of p38-MAPK signaling pathway attenuates breast cancer induced bone pain and disease progression in a murine model of cancer-induced bone pain, *Mol. Pain* 7 (2011) 81.